

Hypervalent Compounds

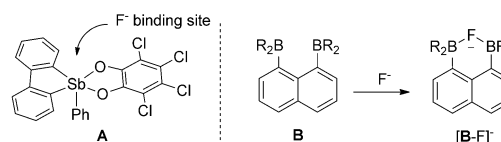
Squeezing Fluoride out of Water with a Neutral Bidentate Antimony(V) Lewis Acid**

Masato Hirai and François P. Gabbaï*

Abstract: Because of hydration, fluoride ions in water typically elude complexation by neutral Lewis acids. Here, we show how this limitation can be overcome with a bidentate Lewis acid containing two antimony(V) centers. This derivative (**2**) is obtained by the simple reaction of 4,5-bis(diphenylstibino)-9,9-dimethylxanthene (**1**) with two equivalents of 3,4,5,6-tetrachlorobenzoquinone (*o*-chloranil). It features two square-pyramidal stiborane units oriented in a face-to-face fashion. Titration experiments show that this new bidentate Lewis acid binds fluoride in aqueous solutions containing 95 % water with a binding constant (*K*) of $700 \pm 30 \text{ M}^{-1}$. The structure of the fluoride adduct confirms fluoride anion chelation between the two antimony centers.

Owing to its small size, the fluoride anion exhibits a high hydration energy of 504 kJ mol^{-1} . Model studies suggest that this stabilization arises from the formation of hydrogen bonds with as many as seven water molecules that can simultaneously reside in the first solvation shell of the anion.^[1] Owing to the stability of this solvation shell, fluoride ions tend to be inert and thus difficult to capture in aqueous media. This inertness constitutes one of the main limitations encountered in the design of water compatible fluoride sensors and captors for applications in drinking water analysis^[2] and ^{18}F positron emission tomography,^[3] respectively. The most successful approaches reported to date are based on the use of cationic compounds whose fluoride affinity is enhanced by Coulombic effects.^[4] This is for example the case for cationic boranes, which have been shown to bind fluoride in water.^[5] By contrast, neutral boranes cannot overcome the elevated hydration energy of the fluoride anion and are thus incompetent for fluoride complexation in aqueous media.^[6] As part of our ongoing interest in this field, we have recently become interested in antimony(V) Lewis acids^[4d,7] such as **A**, a neutral stiborane that displays stronger Lewis acidities than non-fluorinated triarylboranes.^[8] This higher Lewis acidity is reflected by the fact that **A** binds fluoride in THF/H₂O (7:3, v/v) solution with stability constants *K* in the range of 10^4 M^{-1} ,

whereas boranes show no affinity for the anion under such conditions. Despite the strength of the binding, the use of these molecules in solutions that contain a high water content (> 50 % H₂O) has not been established. Potential problems include coordination of water to the vacant antimony binding site compounded with the strong hydration of the fluoride anion which competes with antimony coordination.^[7c,9] Faced with these difficulties, we have decided to investigate strategies to increase the fluoride affinity of these antimony species. Lessons learned from the chemistry of boron-based fluoride receptors have shown that chelating diboranes of type **B** display a markedly enhanced affinity for fluoride anions.^[6d,10] Inspired by these earlier results, we have now decided to investigate the synthesis and properties of bidentate distiboranes.



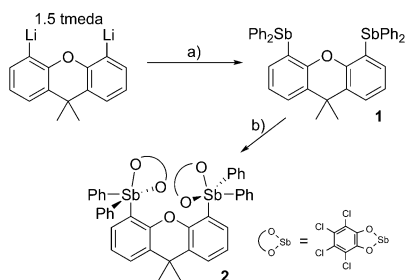
Toward this end, we first prepared 4,5-bis(diphenylstibino)-9,9-dimethylxanthene (**1**) by the reaction of 4,5-dilithio-9,9-dimethylxanthene-1.5(tmeda)^[11] (tmeda = *N,N,N',N'*-tetramethylethane-1,2-diamine) and diphenylantimony chloride (2 equiv). This compound was isolated as a white solid in 60 % yield. Its ^1H NMR spectrum in CDCl₃ indicates that all four phenyl groups are equivalent. The ^1H NMR spectrum also shows the expected dimethylxanthene backbone resonances including three resonances consistent with an ABC spin system arising from the aromatic backbone hydrogen nuclei. The structure of **1** has been confirmed by X-ray diffraction, which shows that the two antimony centers are separated by 4.1517(4) Å (see the Supporting Information, SI).^[12] This new distibine cleanly reacts with *o*-chloranil to afford the corresponding distiborane **2** in 84 % yield (Scheme 1). This distiborane has been fully characterized. In the ^1H NMR spectrum in CDCl₃, the phenyl groups were observed as two broad signals at room temperature, indicating rapid rotation of the phenyl groups in solution. Oxidation of the two antimony centers induces a downfield shift of the dimethylxanthene ABC aromatic spin system resonances which appear at 7.68, 7.11, and 6.78 ppm in **2** versus 7.44, 7.00, and 6.91 ppm in **1**.

Oxidation of the two antimony centers also results in a notable increase of the Sb–Sb separation from 4.1517(4) Å in **1** to 4.7805(7) Å in **2** (Figure 1).^[12] This increase reflects the larger steric bulk of the stiborane units, which both adopt

[*] M. Hirai, Prof. Dr. F. P. Gabbaï
Department of Chemistry, Texas A&M University
College Station, TX 77843 (USA)
E-mail: francois@tamu.edu
Homepage: <http://www.chem.tamu.edu/rgroup/gabbaï/>

[**] Financial support from the Welch Foundation (A-1423), the National Science Foundation (CHE-1300371), Texas A&M University (A. E. Martell Chair), and the Laboratory for Molecular Simulation at Texas A&M University (software and computation resources) is gratefully acknowledged.

Supporting information for this article is available on the WWW under <http://dx.doi.org/10.1002/anie.201410085>.



Scheme 1. Synthesis of **2**. a) 2 equiv Ph_2SbCl , Et_2O , -78°C ; b) 2 equiv *o*-chloranil, THF, RT.

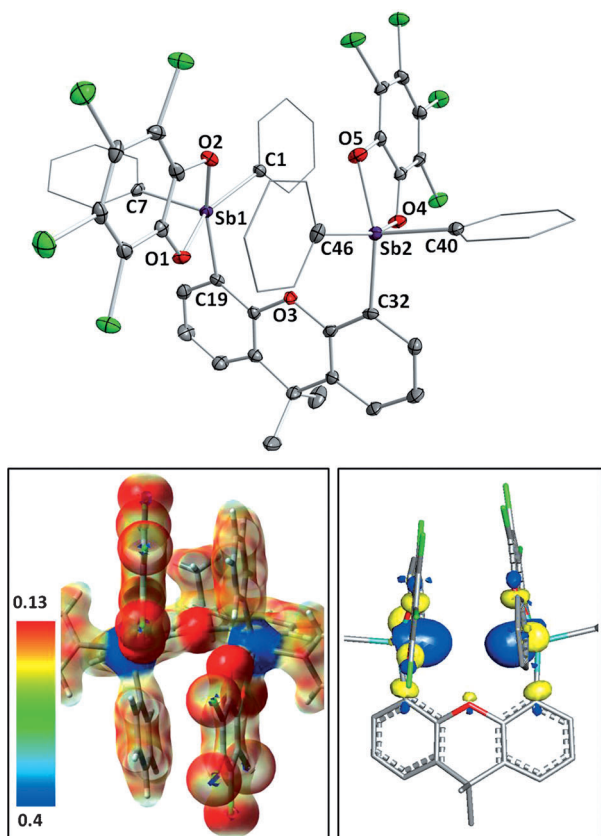
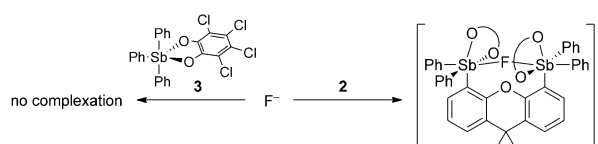


Figure 1. Top: Solid-state structure of the crystallized **2**. Thermal ellipsoids are drawn at the 50% probability level. The hydrogen atoms and toluene molecules are omitted for clarity. Selected bond lengths [Å] and angles [deg]: Sb1–C1 2.115(3), Sb1–C7 2.103(3), Sb1–C19 2.129(3), Sb1–O1 2.0551(18), Sb1–O2 2.0360(18), Sb2–C32 2.134(3), Sb2–C40 2.093(3), Sb2–C46 2.110(3), Sb2–O4 2.0389(18), Sb2–O5 2.0554(18); O1–Sb1–O2 78.46(7), C1–Sb1–C7 102.92(10), C1–Sb1–C19 101.51(10), C7–Sb1–C19 101.51(10), O4–Sb2–O5 78.60(7), C32–Sb2–C40 103.43(10), C32–Sb2–C46 101.35(10), C40–Sb2–C46 107.67(10). Bottom left: electrostatic potential surface of **2** (isovalue = 0.05). Bottom right: Contour plot of the LUMO of **2** (isovalue = 0.05).

a distorted square-pyramidal geometry with an average τ -value of 0.08. In the crystal, the molecule has C_2 symmetry, with the square bases of each pyramid oriented in a face-to-face fashion. This unique arrangement generates a cavity flanked on either side by Lewis acidic antimony(V) atoms. Compound **2** has also been investigated computationally

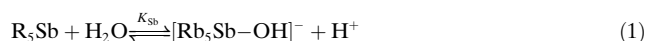
using density functional theory (DFT) methods (B3LYP functional with the mixed basis sets: aug-cc-pVTZ-pp for Sb, 6-311g(d) for Cl, 6-31g for C, O, and H). The electrostatic potential surface of **2** shows an accumulation of positive character at each antimony center. Accordingly, the LUMO is concentrated on the two antimony atoms, which both contribute through orbitals of $\text{Sb}-\text{C}_{\text{ph}}$ σ^* character (Figure 1).

With this compound in hand, we decided to investigate its anion binding properties and compare them to those of $\text{Ph}_3\text{Sb}(\text{O}_2\text{C}_6\text{Cl}_4)$ (**3**), a known derivative which was prepared as a monofunctional model compound for the purpose of this study (Scheme 2).^[13] To make our study more relevant to



Scheme 2. The reaction of fluoride with **2** and **3** in $\text{H}_2\text{O}/\text{THF}$ (9.5:0.5, v/v) solution at pH 4.36 (0.045 M Triton X-100/citrate buffer).

applications that involve aqueous fluoride sources, we decided to evaluate these molecules in solutions with a high water content. We found that both **2** and **3** could be dissolved in $\text{H}_2\text{O}/\text{THF}$ mixtures (9.5:0.5, v/v) in the presence of Triton X-100 (0.045 M), a neutral surfactant often employed as a detergent in biomedical experiments.^[14] To probe the behavior of these two compounds in this solution, we first studied their possible neutralization by hydroxide anions. To this end, we monitored the UV/Vis spectrum of these two compounds as a function of pH. We found that the spectrum of the monofunctional derivative **3** remained unchanged upon increase of the pH from 4 to 6, at which point the band at 308.5 nm undergoes a progressive quenching. Fitting of the titration data to a simple acid–base equilibrium [Eq. (1)] affords $\text{p}K_{\text{Sb}} = 7.40 \pm 0.08$ (see SI).



When the same experiment was carried out with **2**, neutralization started to occur at lower pH leading to a $\text{p}K_{\text{Sb}}$ of 5.77 ± 0.08 (Figure 2).^[15] These measurements are important, because they indicate that **2** is more acidic than **3** by almost two orders of magnitude. Additionally, they clearly demonstrate that the increase in acidity is imparted by the bifunctional nature of **2**. Next, we decided to verify if a similar trend would be observed in the fluoride binding properties of these two compounds. Using the $\text{H}_2\text{O}/\text{THF}$ mixture (9.5:0.5, v/v) described above buffered at pH 4.34 with citrate (0.01 M), we found that incremental addition of fluoride to a solution of **3** (4.3×10^{-5} M) did not result in any changes of the UV/Vis spectrum, thus indicating that monofunctional **3** does not complex fluoride anions under these conditions. By contrast, when the same experiment was repeated with **2** (4.2×10^{-5} M), addition of fluoride induced a notable change of the UV/Vis spectrum, suggesting the formation of a fluoride complex for which a stability constant of $700 \pm 30 \text{ M}^{-1}$ can be calculated

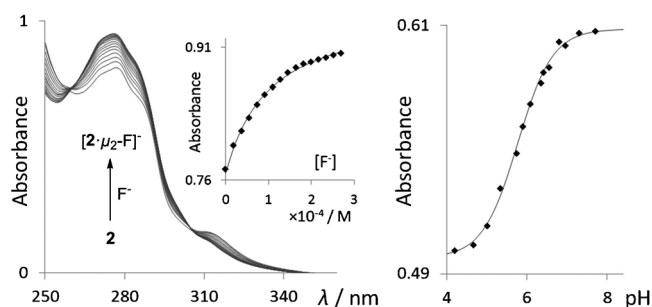
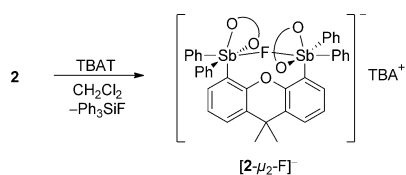


Figure 2. Left: Spectral changes in the UV/Vis absorption spectra of **2** (4.2 × 10⁻⁵ M) in H₂O/THF (9.5:0.5, v/v) solution at pH 4.36 (0.01 M citrate, 0.045 M Triton X-100) upon addition of fluoride. The inset shows the experimental and the calculated 1:1 binding isotherms for **2** at 280.8 nm. The data were fitted with $K = 7.00 \pm 30 \text{ M}^{-1}$ ($\epsilon(\mathbf{2}) = 8850 \text{ M}^{-1} \text{ cm}^{-1}$ and $\epsilon([\mathbf{2}-\mu_2\text{-F}]^-) = 11000 \text{ M}^{-1} \text{ cm}^{-1}$). Right: Spectrophotometric acid-base titration curve of **2** in H₂O/THF (9.5:0.5, v/v) solution (0.01 M sodium phosphate, 0.045 M Triton X-100). The absorbance was measured at 280.8 nm. The data were fitted to $K_{\text{sb}} = \frac{[\mathbf{2}-\mu_2\text{-OH}^-][\text{H}^+]}{[\mathbf{2}]}$ [Eq. (1)] with $\epsilon(\mathbf{2}) = 9700 \text{ M}^{-1} \text{ cm}^{-1}$ and $\epsilon([\mathbf{2}-\mu_2\text{-OH}^-]) = 11850 \text{ M}^{-1} \text{ cm}^{-1}$, and the $\text{p}K_{\text{sb}}$ values estimated as 5.77 ± 0.08 .

(Figure 2). To our knowledge, compound **2** is the first neutral main group Lewis acid to capture fluoride anions in water.^[6d,16] The formation of $[\mathbf{2}-\mu_2\text{-F}]^-$ in these solutions was confirmed by ESI-MS, which shows an intense molecular peak at m/z 1268.7729 amu. No change in the UV/Vis spectrum was observed in the presence of other common anions such as Cl⁻, Br⁻, HCO₃⁻, NO₃⁻, HSO₄⁻, and H₂PO₄⁻, pointing to the selectivity of anion binding.

To confirm that the bidentate nature of **2** is responsible for its increased fluoride anion affinity, we endeavored to isolate a salt containing the anionic complex $[\mathbf{2}-\mu_2\text{-F}]^-$. The tetra-*n*-butylammonium salt of this anion $[\mathbf{2}-\mu_2\text{-F}]^-$ could be easily obtained by reaction of **2** with TBAT ([*n*Bu₄N][Ph₃SiF₂]) in CH₂Cl₂ (Scheme 3). Whereas the ¹H NMR spectrum shows all



Scheme 3. Synthesis of TBA $[\mathbf{2}-\mu_2\text{-F}]$, TBAT = [*n*Bu₄N][Ph₃SiF₂], TBA⁺ = [*n*Bu₄N]⁺.

the expected resonances, the presence of an antimony-bound fluoride anion is revealed by a ¹⁹F NMR signal at -26.5 ppm. The solid-state structure obtained by single-crystal X-ray diffraction^[12] shows that the two antimony centers adopt a distorted octahedral geometry, similar to those of other hexacoordinate antimonate species^[7f,8] including SbF₆⁻ (Figure 3).^[17] Furthermore, the crystal structure confirmed that the fluoride atom is indeed bound to both antimony centers. In agreement with the bridging nature of the fluoride ligand, the Sb–F bonds in **2** (Sb1–F1 2.1684(17) Å, Sb2–F1 2.1622(18) Å) are significantly longer than the Sb–F bond in

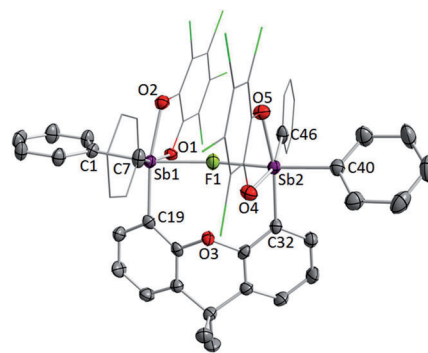


Figure 3. Solid-state structure of the crystallized $[\mathbf{2}-\mu_2\text{-F}]^-$. Thermal ellipsoids are drawn at the 50% probability level. The hydrogen atoms, TBA cation, and THF molecules are omitted for clarity. Selected bond lengths [Å] and angles (deg): Sb1–F1 2.1684(17), Sb2–F1 2.1621(18), Sb1–C1 2.147(3), Sb1–C7 2.137(3), Sb1–C19 2.162(3), Sb1–O1 2.074(2), Sb1–O2 2.071(2), Sb2–C32 2.145(3), Sb2–C40 2.141(3), Sb2–C46 2.132(3), Sb2–O4 2.041(2), Sb2–O5 2.070(2); Sb1–F1–Sb2 165.45(9), C1–Sb1–F1 167.78(9), C7–Sb1–O1 164.12(10), C19–Sb1–O2 164.81(9), C40–Sb2–F1 172.89(9), C32–Sb2–O5 165.90(9), C46–Sb2–O4 163.45(10).

$[\mathbf{3}-\text{F}]^-$ (1.973(4) Å), which was isolated as tetra-*n*-butylammonium salt for the purpose of this study (see SI).^[12] The Sb1–F1–Sb2 angle (165.45(9)°) indicates a slight bending at the fluorine atoms. A similar Sb–F–Sb motif is found in Sb₂F₁₁⁻, a highly stable inorganic anion, which is compatible with strongly acidic environments.^[18] Additionally, the Sb1–Sb2 distance significantly decreases from 4.7805(7) Å in **2** to 4.2957(12) Å in $[\mathbf{2}-\mu_2\text{-F}]^-$, thus illustrating the flexibility of the xanthene backbone and its ability to clamp down on the anionic guest. Strikingly, the distance between F1 and O3 of the xanthene backbone is 2.602(12) Å, which is well within the sum of the van der Waals radii of the two elements (3.05 Å).^[19] Given the fact that an interaction between an oxygen atom and a fluorine atom should be repulsive, we propose that the compression observed in the F1–O3 distance is reflective of the strength of the fluoride chelate effect.

The structure of $[\mathbf{2}-\mu_2\text{-F}]^-$ strongly supports the notion that the higher fluoride affinity of **2** originates from its ability to chelate the fluoride anion. This view is supported by the computed fluoride ion affinity (FIA) of **2** and **3** (FIA = 359.88 kJ mol⁻¹ for **2** and 192.23 kJ mol⁻¹ for **3**) which shows that the chelate Sb–F–Sb motif in $[\mathbf{2}-\mu_2\text{-F}]^-$ is stabilized by more than 160 kJ mol⁻¹ when compared to the terminal Sb–F bond of $[\mathbf{3}-\text{F}]^-$. Accordingly, NMR spectroscopy shows that $[\mathbf{3}-\text{F}]^-$ reacts with **2** to afford $[\mathbf{2}-\mu_2\text{-F}]^-$. A similar reaction is obtained upon mixing **2** with (Mes₂BF)C₆H₄(PPh₂Me) thus indicating that **2** is more Lewis acidic than the cationic borane [*p*-(Mes₂B)C₆H₄(PPh₂Me)]⁺ which we have previously used to complex fluoride ions in water.^[5a] Because the computed FIA of **2** is lower than that of B(C₆F₅)₃ (413.30 kJ mol⁻¹),^[20] we also decided to test the stability of $[\mathbf{2}-\mu_2\text{-F}]^-$ in the presence of this perfluorinated borane. As anticipated from the FIAs, the addition of B(C₆F₅)₃ to a solution of TBA $[\mathbf{2}-\mu_2\text{-F}]$ in CDCl₃ affords quantitative formation of **2** and [BF(C₆F₅)₃]⁻. This reaction occurs without decomposition of **2**, thus indicating that fluoride binding by **2** is reversible.

In conclusion, we report a neutral bidentate distiborane which readily overcomes the hydration of fluoride anions in water. Fluoride complexation, which is highly selective, is driven by the formation of a Sb-F-Sb chelate motif, the existence of which has been established crystallographically. Finally, the importance of bifunctionality is established by a comparison with a monofunctional analogue, which shows that the bidentate distiborane is more acidic by at least two orders of magnitude.

Experimental Section

Synthesis of 1. A solution of Ph_2SbCl (3.52 g, 11.2×10^{-3} mol) in Et_2O (20 mL)/THF (10 mL) was added dropwise to a suspension of 4,5-dilithio-9,9-dimethylxanthene-1.5(tmeda) (2.24 g, 5.6×10^{-3} mol) in Et_2O (30 mL) at -78°C . After stirring at this temperature for an hour, the solution was slowly warmed up to ambient temperature and stirred for an additional 12 h. After adding a drop of water to quench the reaction, the solvent was removed in vacuo and CH_2Cl_2 /hexanes (20 mL/10 mL) was added to the residue. The resulting mixture was stirred over anhydrous MgSO_4 for 30 min before filtering over Celite. The filtrate was concentrated in vacuo and washed with MeOH (15 mL) to afford the product as a white solid in 60% yield (2.55 g, 3.4×10^{-3} mol). Single crystals of **1** were obtained as colorless blocks by slow diffusion of pentane into a THF solution at ambient temperature. ^1H NMR (399.508 MHz, CDCl_3): δ = 7.44 (dd, 2H, $^3J_{\text{H-H}} = 7.8$ Hz, $^4J_{\text{H-H}} = 1.2$ Hz, xanthene-CH), 7.39–7.33 (m, 8H, SbPh), 7.31–7.22 (m, 12H, SbPh), 7.00 (pseudo t, 2H, $^3J_{\text{H-H}} = 7.6$ Hz, xanthene-CH), 6.91 (dd, 2H, $^3J_{\text{H-H}} = 7.2$ Hz, $^4J_{\text{H-H}} = 1.2$ Hz, xanthene-CH), 1.68 ppm (singlet, 6H, xanthene-CH₃). $^{13}\text{C}\{^1\text{H}\}$ NMR (100.466 MHz, CDCl_3): δ = 153.60, 138.87, 136.69, 133.69, 134.94, 129.84, 128.89, 128.49, 127.18, 126.99, 124.55, 34.87 (xanthene-CH₃), 32.55 ppm (xanthene-CH₃). m.p. 132°C . Elemental analysis calculated (%) for $\text{C}_{39}\text{H}_{32}\text{OSb}_2$: C, 61.62; H, 4.24; found C, 61.34; H, 4.39.

Synthesis of 2. To a stirred solution of **1** (0.350 g, 4.6×10^{-4} mol) in THF (5 mL) was added a solution of *o*-chloranil (0.226 g, 9.2×10^{-4} mol) in THF (3 mL) dropwise over 10 min. After stirring for 30 min, the solvent was removed in vacuo and washed with two portions of methanol (10 mL each) to afford the product as a pale yellow solid in 86% yield (0.496 g, 4.0×10^{-4} mol). Single crystals of **2** were obtained as yellow blocks by slow diffusion of pentane into a toluene solution at ambient temperature. ^1H NMR (399.508 MHz, CDCl_3): δ = 7.68 (dd, 2H, $^3J_{\text{H-H}} = 7.6$ Hz, $^4J_{\text{H-H}} = 1.6$ Hz, xanthene-CH), 7.60 (broad, 8H, *o*-SbPh), 7.24 (broad, 12H, SbPh), 7.11 (pseudo t, 2H, $^3J_{\text{H-H}} = 8.0$ Hz, xanthene-CH), 6.78 (dd, 2H, $^3J_{\text{H-H}} = 7.2$ Hz, $^4J_{\text{H-H}} = 1.6$ Hz, xanthene-CH), 1.82 ppm (s, 6H, xanthene-CH₃). $^{13}\text{C}\{^1\text{H}\}$ NMR (100.466 MHz, CDCl_3): δ = 152.24, 144.08, 134.22 (broad), 132.83, 131.75 (broad), 131.49, 129.34 (broad), 129.13, 125.19, 124.76, 120.43, 116.59, 35.07, 32.16 ppm (xanthene-CH₃). m.p. 172°C (dec.). Elemental analysis calculated (%) for $\text{C}_{51}\text{H}_{32}\text{Cl}_8\text{O}_5\text{Sb}_2$: C, 48.93; H, 2.58; found C, 49.05; H, 2.72.

Synthesis of TBA[2- μ_2 -F]. To a solution of **2** (0.103 g, 8.2×10^{-5} mol) in dichloromethane (10 mL) was added a solution of TBAT (0.044 g, 8.2×10^{-5} mol) in dichloromethane (5 mL). After stirring for 15 min, the mixture was treated with water (10 mL). The organic layer was separated, dried with anhydrous MgSO_4 and filtered over Celite. Removal of the solvent in vacuo afforded TBA[2- μ_2 -F] as a white solid which was washed with two portions of Et_2O (5 mL each). This procedure afforded TBA[2- μ_2 -F] in 91% yield (0.113 g, 7.5×10^{-5} mol). Single crystals of TBA[2- μ_2 -F] were obtained as colorless blocks by slow diffusion of Et_2O into a MeCN solution at ambient temperature. ^1H NMR (499.42 MHz, CDCl_3): δ = 7.65 (d, 4H, $^3J_{\text{H-H}} = 7.5$ Hz, *o*-SbPh), 7.44 (dd, 2H, $^3J_{\text{H-H}} = 7.5$ Hz, $^4J_{\text{H-H}} = 1.5$ Hz, xanthene-CH), 7.24 (pseudo t, 2H, $^3J_{\text{H-H}} = 7.5$ Hz, xanthene-CH), 7.11 (m, 14H, SbPh), 6.91 (t, 2H, $^3J_{\text{H-H}} = 7.5$ Hz, *p*-SbPh), 6.69 (dd, 2H, $^3J_{\text{H-H}} = 7.5$ Hz, $^4J_{\text{H-H}} = 1.5$ Hz, xanthene-CH), 2.52 (m,

8H, TBA-CH₂), 1.76 (s, 6H, xanthene-CH₃), 1.23 (broad, 8H, TBA-CH₂), 1.12 (m, 8H, TBA-CH₂), 0.89 ppm (t, 12H, $^3J_{\text{H-H}} = 7.2$ Hz, TBA-CH₃). $^{13}\text{C}\{^1\text{H}\}$ NMR (125.60 MHz, CDCl_3): δ = 158.35, 147.25, 146.42, 135.96, 134.22, 134.09, 132.72, 132.32, 128.51, 128.40, 127.95, 127.69, 125.30, 123.10, 117.55, 117.22, 115.23, 115.18, 58.85 (TBA-CH₂), 36.78 (xanthene-CH₃), 26.94, 23.85 (TBA-CH₂), 19.66 (TBA-CH₂), 13.71 ppm (TBA-CH₃). ^{19}F NMR (469.86 MHz, CDCl_3): δ = -26.5 (s). m.p. 240°C (dec.). Elemental analysis calculated (%) for $\text{C}_{67}\text{H}_{68}\text{Cl}_8\text{FNO}_5\text{Sb}_2$: C, 53.17; H, 4.53; N, 0.93; found C, 53.16; H, 4.66; N, 0.94. HRMS (ESI-TOFMS): m/z calculated for $\text{C}_{51}\text{H}_{32}\text{Cl}_8\text{FO}_5\text{Sb}_2$ 1270.7764, found 1270.7752.

Received: October 14, 2014

Published online: November 25, 2014

Keywords: antimony · fluoride · hypervalent compounds · Lewis acids · main group elements

- [1] M. Gerken, J. A. Boatz, A. Kornath, R. Haiges, S. Schneider, T. Schroer, K. O. Christe, *J. Fluorine Chem.* **2002**, *116*, 49–58.
- [2] K. Sebelius, *Federal Register* **2011**, *76*, 2383–2388
- [3] T. A. D. Smith, *J. Labelled Compd. Radiopharm.* **2012**, *55*, 281–288.
- [4] a) E. L. Yee, O. A. Gansow, M. J. Weaver, *J. Am. Chem. Soc.* **1980**, *102*, 2278–2285; b) R. Tripier, C. Platas-Iglesias, A. Boos, J.-F. Morfin, L. Charbonnière, *Eur. J. Inorg. Chem.* **2010**, 2735–2745; c) L. M. P. Lima, A. Lecointre, J.-F. Morfin, A. de Blas, D. Visvikis, L. J. Charbonnière, C. Platas-Iglesias, R. Tripier, *Inorg. Chem.* **2011**, *50*, 12508–12521; d) I.-S. Ke, M. Myahkostupov, F. N. Castellano, F. P. Gabbai, *J. Am. Chem. Soc.* **2012**, *134*, 15309–15311; e) H. Zhao, L. A. Leamer, F. P. Gabbai, *Dalton Trans.* **2013**, *42*, 8164–8178; f) A. Brugnara, F. Topic, K. Rissanen, A. d. L. Lande, B. Colasson, O. Reinaud, *Chem. Sci.* **2014**, *5*, 3897–3904.
- [5] a) M. H. Lee, T. Agou, J. Kobayashi, T. Kawashima, F. P. Gabbai, *Chem. Commun.* **2007**, 1133–1135; b) T. W. Hudnall, F. P. Gabbai, *J. Am. Chem. Soc.* **2007**, *129*, 11978–11986; c) Y. Kim, F. P. Gabbai, *J. Am. Chem. Soc.* **2009**, *131*, 3363–3369; d) T. Agou, M. Sekine, J. Kobayashi, T. Kawashima, *Chem. Eur. J.* **2009**, *15*, 5056–5062; e) K. C. Song, K. M. Lee, H. Kim, Y. S. Lee, M. H. Lee, Y. Do, *J. Organomet. Chem.* **2012**, *713*, 89–95.
- [6] a) S. Yamaguchi, S. Akiyama, K. Tamao, *J. Am. Chem. Soc.* **2001**, *123*, 11372–11375; b) Y. Kubo, M. Yamamoto, M. Ikeda, M. Takeuchi, S. Shinkai, S. Yamaguchi, K. Tamao, *Angew. Chem. Int. Ed.* **2003**, *42*, 2036–2040; *Angew. Chem.* **2003**, *115*, 2082–2086; c) S. Yamaguchi, T. Shirasaka, S. Akiyama, K. Tamao, *J. Am. Chem. Soc.* **2002**, *124*, 8816–8817; d) S. Solé, F. P. Gabbai, *Chem. Commun.* **2004**, 1284–1285.
- [7] a) L. H. Bowen, R. T. Rood, *J. Inorg. Nucl. Chem.* **1966**, *28*, 1985–1990; b) M. Jean, *Anal. Chim. Acta* **1971**, *57*, 438–439; c) M. Hall, D. B. Sowerby, *J. Am. Chem. Soc.* **1980**, *102*, 628–632; d) V. A. Dodonov, A. Y. Fedorov, G. K. Fukin, S. N. Zaburdyaeva, L. N. Zakharov, A. V. Ignatenko, *Main Group Chem.* **1999**, *3*, 15–22; e) E. Conrad, N. Burford, R. McDonald, M. J. Ferguson, *J. Am. Chem. Soc.* **2009**, *131*, 17000–17008; f) C. R. Wade, T.-P. Lin, R. C. Nelson, E. A. Mader, J. T. Miller, F. P. Gabbai, *J. Am. Chem. Soc.* **2011**, *133*, 8948–8955; g) C. R. Wade, F. P. Gabbai, *Organometallics* **2011**, *30*, 4479–4481; h) C. R. Wade, I.-S. Ke, F. P. Gabbai, *Angew. Chem. Int. Ed.* **2012**, *51*, 478–481; *Angew. Chem.* **2012**, *124*, 493–496; i) T.-P. Lin, R. C. Nelson, T. Wu, J. T. Miller, F. P. Gabbai, *Chem. Sci.* **2012**, *3*, 1128–1136; j) S. L. Benjamin, W. Levason, G. Reid, R. P. Warr, *Organometallics* **2012**, *31*, 1025–1034; k) I.-S. Ke, J. S. Jones, F. P. Gabbai, *Angew. Chem. Int. Ed.* **2014**, *53*, 2633–2637; *Angew. Chem.* **2014**, *126*, 2671–2675; l) B. Pan, F. P. Gabbai, *J. Am. Chem. Soc.* **2014**, *136*, 9564–9567; m) A. P. M.

- Robertson, N. Burford, R. McDonald, M. J. Ferguson, *Angew. Chem. Int. Ed.* **2014**, 53, 3480–3483; *Angew. Chem.* **2014**, 126, 3548–3551.
- [8] M. Hirai, F. P. Gabbaï, *Chem. Sci.* **2014**, 5, 1886–1893.
- [9] a) T. Tunde Bamgboye, M. J. Begley, D. B. Sowerby, *J. Organomet. Chem.* **1989**, 362, 77–85; b) L.-J. Baker, C. E. F. Rickard, M. J. Taylor, *Acta Crystallogr. Sect. C* **1999**, 55, 335–337.
- [10] a) H. E. Katz, *J. Org. Chem.* **1985**, 50, 5027–5032; b) H. E. Katz, *Inclusion Compd.* **1991**, 4, 391–405; c) H. E. Katz, *J. Am. Chem. Soc.* **1985**, 107, 1420–1421; d) M. Melaïmi, S. Sole, C.-W. Chiu, H. Wang, F. P. Gabbaï, *Inorg. Chem.* **2006**, 45, 8136–8143; e) C. Jiang, O. Blacque, H. Berke, *Chem. Commun.* **2009**, 5518–5520; f) H. Zhao, F. P. Gabbaï, *Organometallics* **2012**, 31, 2327–2335.
- [11] H. Wang, F. P. Gabbaï, *Organometallics* **2005**, 24, 2898–2902.
- [12] CCDC 1027319 (**1**), 1027320 (**2**), 1027321 (TBA[**2**-μ-F]), and 1027322 (TBA[**3**-F]) contain the supplementary crystallographic data for this paper. These data can be obtained free of charge from The Cambridge Crystallographic Data Centre via www.ccdc.cam.ac.uk/data_request/cif.
- [13] R. R. Holmes, R. O. Day, V. Chandrasekhar, J. M. Holmes, *Inorg. Chem.* **1987**, 26, 157–163.
- [14] D. Lichtenberg, H. Ahyayauch, A. Alonso, F. M. Goñi, *Trends Biochem. Sci.* **2013**, 38, 85–93.
- [15] N. C. Deno, J. J. Jaruzelski, A. Schriesheim, *J. Am. Chem. Soc.* **1955**, 77, 3044–3051.
- [16] a) M. Melaïmi, F. P. Gabbaï, *J. Am. Chem. Soc.* **2005**, 127, 9680–9681; b) M. H. Lee, F. P. Gabbaï, *Inorg. Chem.* **2007**, 46, 8132–8138.
- [17] G. J. Krüger, C. W. F. T. Pistorius, A. M. Heyns, *Acta Crystallogr. Sect. B* **1976**, 32, 2916–2918.
- [18] a) D. Zhang, S. J. Rettig, J. Trotter, F. Aubke, *Inorg. Chem.* **1996**, 35, 6113–6130; b) R. J. Gillespie, K. C. Moss, *J. Chem. Soc. A* **1966**, 1170–1175; c) A. Commeyras, G. A. Olah, *J. Am. Chem. Soc.* **1969**, 91, 2929–2942.
- [19] S. S. Batsanov, *Inorg. Mater.* **2001**, 37, 871–885.
- [20] a) I. Krossing, I. Raabe, *Chem. Eur. J.* **2004**, 10, 5017–5030; b) A. Y. Timoshkin, G. Frenking, *Organometallics* **2008**, 27, 371–380; c) H. Zhao, J. H. Reibenspies, F. P. Gabbaï, *Dalton Trans.* **2013**, 42, 608–610.